

DurFlex-EVC: Duration-Flexible Emotional Voice Conversion with Parallel Generation

Hyung-Seok Oh^{id}, Sang-Hoon Lee^{id}, Deok-Hyeon Cho^{id}, and Seong-Whan Lee^{id}, *Fellow, IEEE*

Abstract—Emotional voice conversion (EVC) seeks to modify the emotional tone of a speaker’s voice while preserving the original linguistic content and the speaker’s unique vocal characteristics. Recent advancements in EVC have involved the simultaneous modeling of pitch and duration, utilizing the potential of sequence-to-sequence (seq2seq) models. To enhance reliability and efficiency in conversion, this study shifts focus towards parallel speech generation. We introduce Duration-Flexible EVC (DurFlex-EVC), which integrates a style autoencoder and unit aligner. Traditional models, while incorporating self-supervised learning (SSL) representations that contain both linguistic and paralinguistic information, have neglected this dual nature, leading to reduced controllability. Addressing this issue, we implement cross-attention to synchronize these representations with various emotions. Additionally, a style autoencoder is developed for the disentanglement and manipulation of style elements. The efficacy of our approach is validated through both subjective and objective evaluations, establishing its superiority over existing models in the field.

Index Terms—Emotional voice conversion, self-supervised representation, denoising diffusion model, cross-attention

I. INTRODUCTION

EMOTIONAL voice conversion (EVC) is a process that alters the emotional tone of a voice while preserving the linguistic content and unique characteristics of the speaker. EVC has gained prominence, particularly in the realm of voice-interactive technologies such as virtual assistants and IoT devices, enhancing the human-like and emotionally resonant aspects of digital interactions [1]–[3].

A pivotal challenge in EVC is maintaining the original speaker’s identity and the content of their speech while altering only the speech attributes that convey emotional tones [4], [5]. This necessitates the appropriate adjustment of the voice’s prosody to align with the intended emotion. Prosodic elements, including intonation, rhythm, and energy, play a critical role in both conveying and recognizing emotions in speech. Despite the intuitive nature of controlling prosody for emotion conversion [6], fine-tuning each prosodic component poses significant challenges.

This work was supported by Institute of Information & communications Technology Planning & Evaluation (IITP) grant funded by the Korea government (MSIT) (No. 2019-0-00079, Artificial Intelligence Graduate School Program (Korea University) and No. 2021-0-02068, Artificial Intelligence Innovation Hub) (*Corresponding author: Seong-Whan Lee.*)

H.-S. Oh, S.-H. Lee, D.-H. Cho and S.-W. Lee are with the Department of Artificial Intelligence, Korea University, 145, Anam-ro, Seongbuk-gu, Seoul 02841, Republic of Korea. E-mail: (hs_oh@korea.ac.kr sh_lee@korea.ac.kr dh_cho@korea.ac.kr sw.lee@korea.ac.kr)

The field of EVC has been revolutionized by advancements in deep learning [7], [8]. Early methodologies employed Gaussian mixture models [9] for converting spectral and prosodic features to produce more expressive voices. Subsequent developments led to autoencoder-based methods [10]–[12], enabling learning in non-parallel data-driven EVC. Particularly, VAE-based methods [13], such as the hybrid VAE-GAN model [13], have been crucial for converting non-parallel emotional speech without altering the speaker’s identity and linguistic content. GAN-based approaches [14], [15], utilizing frameworks such as Cycle-GAN [16], StarGAN [17], and VAE-GAN [18], represent further advancements. However, these methods primarily facilitate emotion conversion at a fixed length, overlooking rhythm’s essential role in emotion.

Sequence-to-sequence (Seq2Seq)-based models, capable of implicitly modeling duration, have emerged as a significant development [19], [20]. These models often adopt specific strategies, such as a two-stage learning strategy integrating a text-to-speech (TTS) model, to enhance learning stability [21], [22]. While seq2seq models can generate varying durations, they face typical autoregressive model challenges, such as long-term dependency and repetition issues, necessitating a parallel generation approach for efficiency and reliability.

Recently, the exploration of discrete speech units through self-supervised learning representations has shown promise in addressing parallel generation challenges in speech processing. This technique encodes speech into discrete units, facilitating frame-level duration extraction for each unit. Certain studies [23], [24] have investigated leveraging these properties. For instance, [23], [24] proposed an approach akin to spoken language translation for speech emotion conversion, enabling parallel audio generation by predicting the duration of each unit. However, this approach does not fully achieve parallel generation due to its reliance on autoregressive models for emotion translation.

To address these limitations, this paper focuses on managing duration control and facilitating emotional context transitions within parallel generation models. The primary contributions of our research are as follows:

- Introduction of a duration-flexible EVC (DurFlex-EVC) that supports fully parallel generation.
- Development of a style autoencoder to enhance style control through decomposition and reassembly of styles.
- Creation of a unit aligner to model unit durations and generate unit-level context vectors.
- Demonstrated superiority of DurFlex-EVC over compar-

tive models through subjective and objective evaluations.

II. BACKGROUND

A. Exploring Self-Supervised Learning in Speech

Self-supervised learning (SSL) is a machine learning paradigm wherein models are trained on their own datasets to create meaningful representations. This method is particularly beneficial in speech processing, where data labeling can be both time-consuming and costly. The wav2vec 2.0 model [25] utilized contrastive learning to validate SSL representations. The vq-wav2vec model [26] introduced a technique for learning discrete audio representations through self-supervised context prediction and quantization. XLS-R [27] is an extensive cross-lingual speech representation model that builds upon wav2vec 2.0. Hidden-unit BERT (HuBERT) [28] employs a masked prediction approach akin to BERT [29] for learning representations. ContentVec [30] enhances speaker disentanglement within the HuBERT framework. Efforts have also been made to create representations suitable for universal downstream tasks [31], [32].

SSL representations have recently been extensively applied to various downstream tasks, such as automatic speech recognition [25], voice conversion [33], [34], speaker verification [35], speech synthesis [36], speech emotion recognition [37], and speech enhancement [38], [39].

B. Discrete Units in Speech Processing

In the realm of audio and speech, discrete unit representation has been proposed for diverse tasks. SoundStream [40] introduced a neural audio codec employing a residual vector quantizer (RVQ), while EnCodec [41] focuses on high-fidelity audio compression and lightweighting through similar methods. UniAudio [42] emerged as a general-purpose audio generation model. These neural codec-based methods, aimed primarily at audio compression and restoration, feature large codebooks and relatively small dimensions.

Conversely, certain methods emphasize compressing speech into semantic units. A method to decompose and reconstruct speech into discrete units of pitch and speaker characteristics was proposed [43]. Building upon this, soft speech units were suggested [23] for enhanced content capture, thus improving speech conversion’s naturalness and intelligibility. Additionally, speech emotion conversion was explored as a language translation task [44], using discrete representations of phonetic content, prosody, speaker, and emotion, in conjunction with a neural vocoder for speech waveform generation. UnitSpeech [24] demonstrated proficiency in personalized TTS and voice conversion, fine-tuning a diffusion-based TTS model with minimal data using self-supervised units, eliminating the need for retraining for each task. Here, semantic speech units serve as content in speech decomposition.

C. Duration Modeling in Speech Processing

Duration modeling is a critical aspect of speech synthesis, particularly in TTS, where mismatches between character length and signals can occur. Early TTS methods addressed

this through autoregressive models with implicit duration modeling, generating one frame at a time [45], [46]. FastSpeech [47] leveraged the encoder-decoder attention alignment of an autoregressive teacher model to model phoneme duration, facilitating parallel generation. FastSpeech 2 [48] introduced a method for extracting phoneme duration from forced external alignment. Glow-TTS [49] developed a technique for identifying the most similar monotonic alignment between text and latent using a monotonic alignment search. Duration modeling advancements have also been applied to voice conversion, with seq2seq models handling duration changes [50], [51]. The DCVC model [52] utilized a phoneme-based information bottleneck for style transfer and speech speed control in voice conversion. Discrete speech units have been employed [24], [43] to model duration through consecutive unit counts. In EVC, a trend towards seq2seq structures for handling duration changes has been observed [21], [22], [53]. However, despite [44] proposing EVC using units for parallel generation, it still relies on the seq2seq model for the unit translation process.

III. PROPOSED METHOD

In this research, we introduce the DurFlex-EVC model, innovatively designed for parallel generation with enhanced duration flexibility. This model is intricately structured, comprising five key components:

- 1) A feature extractor that adeptly transforms raw audio waveforms into finely processed features.
- 2) A style autoencoder, facilitating the decomposition of content and style.
- 3) A unit aligner, responsible for context transformation and meticulous duration modeling.
- 4) A hierarchical stylization encoder, operating at both unit and frame levels for nuanced stylization.
- 5) A diffusion-based generator, engineered for the generation of high-quality Mel-spectrograms.

Fig. 1 illustrates the comprehensive framework of DurFlex-EVC, with detailed explanations provided in the subsequent subsections.

A. Overview

Initially, the model processes the raw waveform using a feature extractor, preparing it as input. This extractor is crucial in converting raw audio waveforms into processed features, such as Mel-spectrograms or SSL representations. In our methodology, HuBERT [28] is employed as the feature extractor, utilizing the output from its final layer as the input features. Following this, the style autoencoder decomposes the style from these representations and reconstructs it. The unit aligner then aggregates contextual information at the frame level through a cross-attention module. This representation undergoes compression to the unit level, feeding into the hierarchical stylization encoder. This encoder adeptly stylizes the latent information at the unit level, expands it, and applies further stylization at the frame level, thus exemplifying the model’s innovative design. The diffusion-based generator creates a Mel-spectrogram through the hierarchical stylization

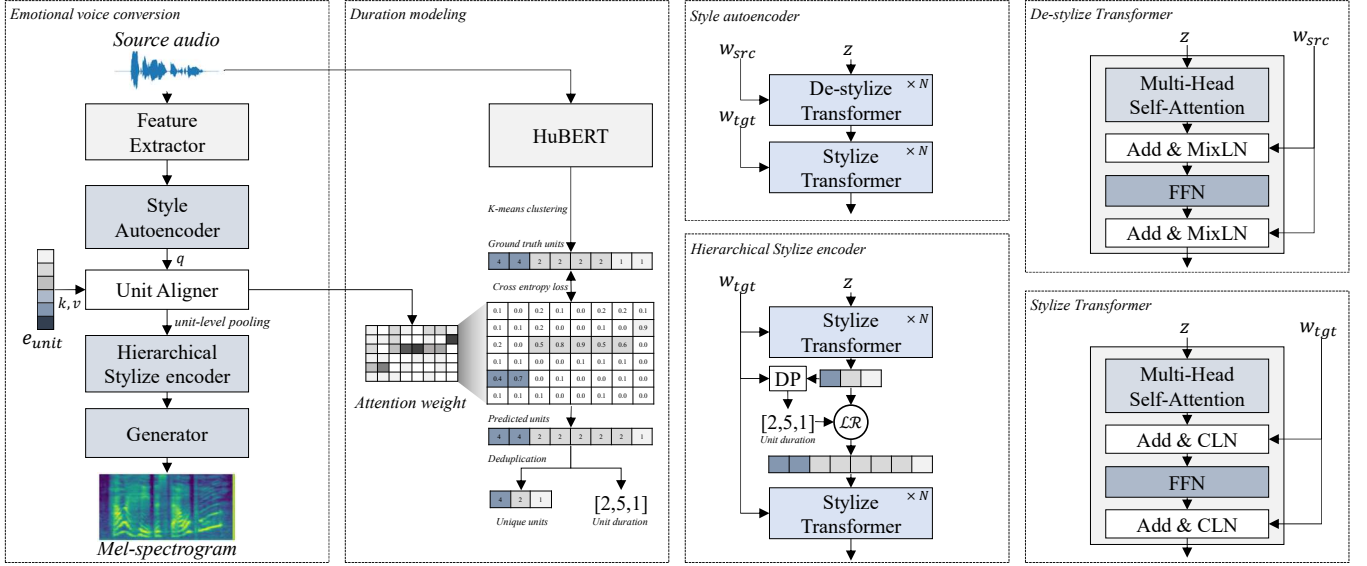


Fig. 1. Overall framework of the proposed method. The feature extractor transforms the source audio into input features. These features are subsequently disentangled and reconditioned by the style autoencoder. The unit aligner is responsible for providing unit-level context and performing duration modeling. In addition, the hierarchical style encoder encodes features at both the unit and frame levels. Mel-spectrograms are subsequently produced by the generator. In this figure, “DP” represents the duration predictor, \mathcal{LR} denotes the length regulator, while “q”, “k”, and “v” represent the query, key, and value of the cross-attention in the unit aligner, respectively.

encoder’s output and a style vector. Subsequently, this Mel-spectrogram undergoes conversion into a raw waveform via a pre-trained vocoder.

B. Style Autoencoder

The style autoencoder, innovatively structured to disentangle and manipulate style effectively, encompasses two primary components: the de-stylization transformer and the stylization transformer. These components were developed employing sophisticated normalization techniques.

Firstly, layer normalization (LN) serves as a fundamental technique, mathematically expressed as follows:

$$\text{LN}(z) = \frac{z - \mu}{\sigma}, \quad (1)$$

where z represents the input vector to be normalized, μ is the mean of the vector, and σ is its standard deviation. LN offers a standardized baseline for processing input, which is critical for consistent style manipulation.

The stylization transformer employs conditional layer normalization (CLN) [54] based on LN to adapt styles effectively. CLN is defined as follows:

$$\text{CLN}(z, w) = \gamma(w) \times \text{LN}(z) + \beta(w), \quad (2)$$

where $\gamma(w)$ and $\beta(w)$ are adaptive parameters representing the gain and bias for the style vector w .

In contrast, the de-stylization transformer employs mix-style layer normalization (MixLN) [55], an adaptation of CLN, to isolate style-independent features. MixLN introduces perturbations into the input directed towards the style vector, inhibiting the model’s tendency to learn style-specific features.

This perturbation is executed by blending the original style vectors with batch-level shuffled style vectors.

$$\gamma_{mix}(w) = \lambda\gamma(w) + (1 - \lambda)\gamma(\tilde{w}), \quad (3)$$

$$\beta_{mix}(w) = \lambda\beta(w) + (1 - \lambda)\beta(\tilde{w}), \quad (4)$$

where w and \tilde{w} denote the original and shuffled style vectors, respectively. The parameter λ , instrumental in maintaining equilibrium between the original and shuffled styles within the model, adheres to a Beta distribution, $\text{Beta}(\alpha, \alpha)$. This parameter resides in a B -dimensional real number space, denoted as \mathbb{R}^B , wherein B represents the batch size, the quantity of data simultaneously processed by the model. The variable α , spanning from 0 to infinity, plays a crucial role in shaping the behaviour of λ . Therefore, MixLN is defined as follows:

$$\text{MixLN}(z, w) = \gamma_{mix}(w) \times \text{LN}(z) + \beta_{mix}(w). \quad (5)$$

A style autoencoder is composed of a stack consisting of N de-stylization transformers and N stylization transformers, respectively. We constructed the source style vector w_{src} as the sum of the speaker vector s_{src} and the emotion vector e_{src} , and the target style vector w_{tgt} as the sum of the speaker vector s_{src} and the emotion vector e_{tgt} .

$$w_{src} = s_{src} + e_{src}, \quad (6)$$

$$w_{tgt} = s_{src} + e_{tgt}. \quad (7)$$

The speaker vector s_* and emotion vector e_* are obtained from the embedding lookup table. The de-stylization transformer uses w_{src} to disentangle the source style, whereas the stylization transformer utilizes w_{tgt} to apply the target style.

This architecture enables the style autoencoder to effectively decompose and reconstruct styles, enhancing its capability in style manipulation capabilities.

C. Unit Aligner

The unit aligner is designed for semantic modeling. Although the output of the style autoencoder encapsulates both style and content, it is primarily a frame-level representation. To semantically cluster latent representations, we utilize a cross-attention module to generate an attention map, highlighting focused tokens in each frame of the representation. The number of consecutive units used as the duration. We use the output of the style autoencoder as a query (Q) and introduce learnable embeddings e_{unit} as keys (K) and values (V) to cross-attention based on [56]. The attention weights \mathcal{A}_{unit} are computed as follows:

$$\mathcal{A}_{unit} = \text{softmax}\left(\frac{QK^T}{\sqrt{d}}\right), \quad (8)$$

where d is the dimension of Q and K . These weights \mathcal{A}_{unit} are subsequently integrated with the value matrix V to produce the attention output z_{attn} .

$$z_{attn} = \mathcal{A}_{unit} \cdot V. \quad (9)$$

We introduce an additional loss term to guide the attention module to learn semantic information. This approach implies a direct classification task, correlating the attention weights \mathcal{A}_{unit} with the target unit sequence y .

$$\mathcal{L}_{unit} = -\frac{1}{L} \sum_{i=1}^L \sum_{j=1}^C y_{i,j} \log(\mathcal{A}_{unit}^{i,j}), \quad (10)$$

where L is the length of unit sequence, C is the number of unit classes, $\mathcal{A}_{unit}^{i,j}$ represents the predicted probability of the i -th element for class j from the attention weights \mathcal{A}_{unit} , and $y_{i,j}$ is the one-hot encoded class label for the i -th unit for class j . We adopted the HuBERT unit as our target unit.

D. Duration Modeling

The unit sequence can be predicted by identifying the focus of the attention module.

$$\hat{y}_i = \arg \max(\mathcal{A}_{unit}^i), \quad (11)$$

where \hat{y}^i is the i -th predicted unit, and \mathcal{A}_{unit}^i is the i -th frame of the attention weight. To extract a distinct sequence of units and their consecutive counts, a deduplication operation is applied, represented as:

$$\hat{y}_{uniq}, n_{count} = \text{dedup}(\hat{y}), \quad (12)$$

where \hat{y}_{uniq} and n_{count} denote the unique units and their consecutive counts, respectively. For example, given an input sequence $\hat{y} = [4, 4, 2, 2, 2, 2, 1, 1]$, the deduplication operation results in $\hat{y}_{uniq} = [4, 2, 1]$ and $n_{count} = [2, 4, 2]$. This implies two units with index 4, followed by four units with index 2 and two units with index 1. We train the duration predictor with

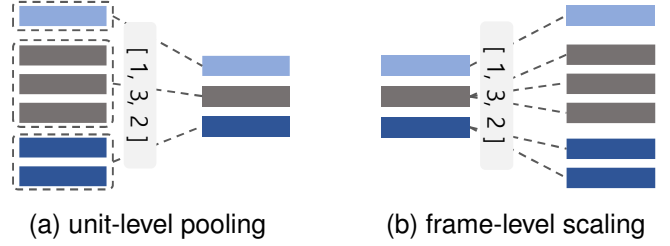


Fig. 2. Unit-level pooling and frame-level scaling. (a) Latent is pooled on average based on unit durations, and (b) Latent is expanded by being duplicated a number of times corresponding to the duration count.

TABLE I
PERFORMANCE OF THE PRE-TRAINED EVALUATOR MODEL ON TEST SETS.

Model	UTMOS	PER (↓)	CER (↓)	WER (↓)	ECA (↑)	SECS (↑)
GT	3.60	11.64	3.06	12.09	81.33	81.46
GT (vocoded)	3.58	11.73	3.14	12.45	81.13	81.04

n_{count} as the target duration. This duration is used to perform unit-level pooling to semantically bundle the output of the unit aligner. Fig. 2a explains unit-level pooling. The output of the unit aligner, z_{attn} , is averaged based on the duration of the unit and results in downsampling the sequence length for alignment at the unit level.

$$z_u = \text{unit-level pool}(z_{attn}, n_{count}), \quad (13)$$

where z_u is the latent downsampled at the unit level. For example, given that $z_{attn} = [0.2, 0.2, 0.1, 0.4, 0.5, 0.2, 0.3, 0.5]$ and $n_{count} = [2, 4, 2]$, the result of unit-level pooling is $z_u = [0.2, 0.3, 0.4]$.

E. Hierarchical Stylization Encoder

The hierarchical stylization encoder [57] functions at two levels: unit level and frame level. It consists of two components: the unit-level stylization transformer (UST) and the frame-level stylization transformer (FST). The UST processes z_u into a z_{us} , denoted as $z_{us} = \text{UST}(z_u, w_{tgt})$, focusing on unit-specific features. This refined variable z_u is scaled to the frame level through a length regulator \mathcal{LR} , depicted in Fig. 2b.

$$z_f = \mathcal{LR}(z_{us}, n_{count}), \quad (14)$$

where z_f represents the latent variable at the frame level. For example, if $z_{us} = [0.1, 0.2, 0.5]$ and $n_{count} = [2, 5, 1]$, then z_f becomes $[0.1, 0.1, 0.2, 0.2, 0.2, 0.2, 0.2, 0.5]$. The FST further refines the frame-level features z_f into z_{fs} , expressed as $z_{fs} = \text{FST}(z_f, w_{tgt})$. This final output z_{fs} is subsequently used as input for the Mel-spectrogram generator.

The duration predictor takes z_{us} and w_{tgt} as input and is trained to predict the unit-level duration n_{count} . For emotion-based duration dynamics, we introduce the flow-based stochastic duration predictor proposed in [58] to introduce duration uncertainty. The duration predictor training objective \mathcal{L}_{dur} follows a negative variational lower bound.

F. Diffusion-Based Mel-Spectrogram Synthesis Generator

Recent progress in speech synthesis has shown that diffusion-based techniques excel in producing high-quality Mel-spectrograms. Our methodology leverages a diffusion framework, anchored in stochastic differential equations (SDEs), which is specifically tailored for Mel-spectrogram synthesis.

The diffusion-based speech synthesis model delineates a forward process, progressively converting the Mel-spectrogram X_0 into Gaussian noise $X_T \sim \mathcal{N}(0, I)$. Data generation occurs through a reverse process. In our model, a standard normal distribution serves as the prior, aligning with the strategy outlined in [24]. The forward process is defined as follows:

$$dX_t = -\frac{1}{2}\beta(t)X_t dt + \sqrt{\beta(t)}dW_t, \quad (15)$$

where $\beta(t)$ is the pre-defined noise schedule, and dW_t is the standard Wiener process. This process adds noise to the initial state X_0 , progressively leading to a Gaussian noise distribution.

During forward diffusion process, the transition of the initial state X_0 into X_t is represented by

$$X_t = \sqrt{1 - \lambda(t)}X_0 + \sqrt{\lambda(t)}\xi_t, \quad (16)$$

where $\lambda(t) = 1 - e^{-\int_0^t \beta(s)ds}$. ξ_t is sampled from $\mathcal{N}(0, I)$ and t ranges from 0 to 1.

The reverse process concentrates on reconstructing the Mel-spectrogram state from its distorted version caused by noise. The reverse diffusion is described by

$$dX_t = -\frac{1}{2}\beta(t)X_t dt - \beta(t)\nabla_{X_t} \log p_t(X_t) dt + \sqrt{\beta(t)}d\widetilde{W}_t, \quad (17)$$

where $\nabla_{X_t} \log p_t(X_t)$ represents the score function, and \widetilde{W}_t denotes the reverse-time Wiener process. The score is given as

$$\nabla_{X_t} \log p_t(X_t|X_0) dt = -\frac{\xi_t}{\lambda(t)}, \quad (18)$$

For score estimation, our model incorporates a network, denoted s_θ , based on the U-net architecture with linear attention, similar to the method used in Grad-TTS [59]. The network is trained with the following loss function:

$$\mathcal{L}_{diff} = \mathbb{E}_{t, X_0, \xi_t} \left[\left\| s_\theta(X_t, t, z_{fs}, w_{tgt}) - \frac{\xi_t}{\lambda(t)} \right\|_2^2 \right]. \quad (19)$$

The model generates data through a discrete inverse process, and the conversion from X_t to $X_{t-\frac{1}{N_{step}}}$ is as follows:

$$X_{t-\frac{1}{N_{step}}} = X_t + \frac{\beta(t)}{N_{step}} \left(\frac{1}{2}X_t + \nabla_{X_t} \log p_t(X_t) \right) + \sqrt{\frac{\beta(t)}{N_{step}}}z_t, \quad (20)$$

where N_{step} represents the number of sampling steps, and $z_t \sim \mathcal{N}(0, I)$ represents Gaussian noise.

G. Training Objective

Consequently, the model is trained using the following loss function:

$$\mathcal{L}_{total} = \mathcal{L}_{diff} + \mathcal{L}_{unit} + \mathcal{L}_{dur}. \quad (21)$$

IV. EXPERIMENTS

A. Experimental Setup

We conducted experiments using the emotional speech dataset (ESD) ¹ [60] containing 350 parallel utterances spoken by 10 native Mandarin speakers and 10 English speakers with 5 emotional states (neutral, happy, angry, sad, and surprise). Following the data partitioning guidelines provided in ESD, the training set was compiled with 300 samples for each emotion per speaker, totaling 15,000 samples. The validation set included 20 samples for each emotion per speaker, totaling 1,000 samples, while the test set comprised 30 samples for each emotion per speaker, totaling 1,500 samples. We sampled audio at 16,000 Hz and transformed it to an 80-bin Mel-spectrogram using an STFT with a window length of 1,024 and a hop size of 256.

B. Implementation Details

In our experimental setup, we configured both the de-stylization and stylization transformers with specific parameters: the hidden dimension, kernel size, number of heads, FFN kernel size, and FFN hidden size were set to 256, 5, 2, 9, and 1024, respectively. The α parameter of the Beta distribution for MixLN was fixed at 0.1. All transformers employed in our model were organized into N layers, with N established at 4. The unit aligner featured multi-head attention with 16 heads. We set $T = 1$, $\beta_t = \beta_0 + (\beta_1 - \beta_0)t$, $\beta_0 = 0.05$, and $\beta_1 = 20$ as noise schedules. The U-Net in our model was set to downsample four times and had a hidden dimension of 128. The timestep N_{step} for inference was designated as 100. The duration predictor, comprising residual blocks utilizing dilated and depth-separable convolution, was structured in four layers. To address the resolution disparity between the HuBERT unit and the Mel-spectrogram, we expanded the hidden representation with a length regulator and employed linear interpolation for upsampling. In training the generator, we utilized random segments, setting the segment size to 32 frames of the Mel-spectrogram. The AdamW optimizer [61] was used, with a learning rate of 1×10^{-4} . The batch size throughout the training was maintained at 16, and the training duration extended to 500K steps. We trained the vocoder using the official BigVGAN-large ² [62] implementation, incorporating LibriTTS [63], VCTK ³, and ESD datasets. All comparison models were trained using a single NVIDIA RTX A6000 GPU. For broader accessibility, the code⁴ and a demo⁵ of our proposed method are available online.

¹<https://github.com/HLTSingapore/Emotional-Speech-Data>

²<https://github.com/NVIDIA/BigVGAN>

³<https://datashare.ed.ac.uk/handle/10283/2651>

⁴<https://github.com/hs-oh-prml/DurFlexEVC>

⁵<https://prml-lab-speech-team.github.io/durflex/>

TABLE II
RESULTS OF SUBJECTIVE AND OBJECTIVE EVALUATIONS FOR EACH COMPARISON MODEL.

Model	Subjective evaluation			Objective evaluation					
	nMOS (\uparrow)	sMOS (\uparrow)	eMOC (\uparrow)	UTMOS	PER (\downarrow)	CER (\downarrow)	WER (\downarrow)	ECA (\uparrow)	SECS (\uparrow)
GT	3.72 (± 0.03)	3.95 (± 0.06)	82.98	-	-	-	-	-	-
GT (vocoded)	3.70 (± 0.05)	3.58 (± 0.11)	82.98	-	-	-	-	-	-
StarGAN-EVC	3.59 (± 0.06)	3.36 (± 0.12)	37.84	1.47	70.83	44.49	67.71	64.75	61.31
Seq2seq-EVC	3.43 (± 0.07)	3.09 (± 0.13)	48.65	1.54	37.29	21.68	36.87	73.11	62.52
Emovox	3.50 (± 0.06)	3.10 (± 0.13)	51.35	2.05	29.25	17.18	31.37	81.13	68.44
Mixed Emotion	3.50 (± 0.07)	3.27 (± 0.12)	62.16	2.02	29.86	18.21	33.09	87.43	66.71
Textless-EVC	3.61 (± 0.05)	3.39 (± 0.11)	56.76	2.37	22.88	12.49	23.98	58.45	68.01
DurFlex-EVC	3.70 (± 0.05)	3.63 (± 0.10)	72.97	3.58	17.31	8.26	20.75	91.58	74.83

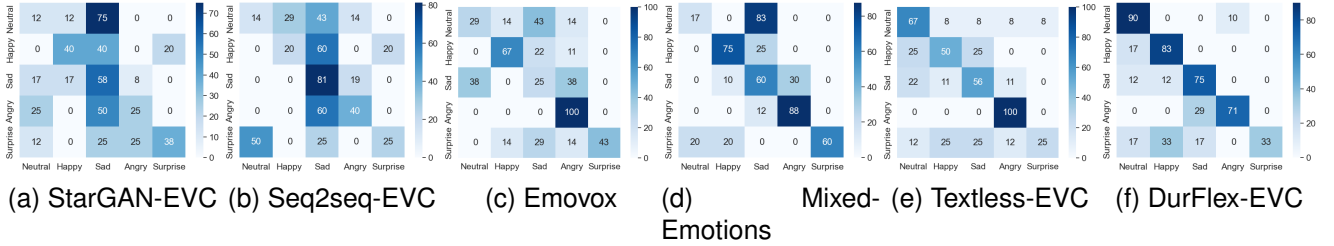


Fig. 3. Confusion matrix of eMOC for each comparison model.

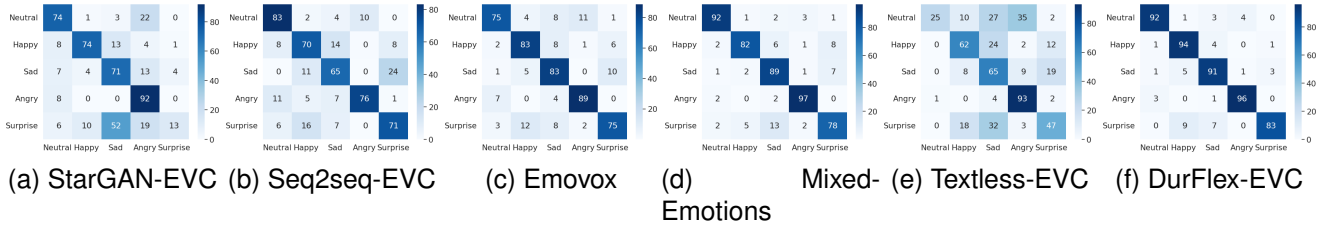


Fig. 4. Confusion matrix of ECA for each comparison model.

C. Evaluation

1) *Subjective Metrics*: We conducted subjective evaluations using Amazon Mechanical Turk (mTurk). Our analysis included the mean opinion score (MOS) for naturalness (nMOS) and speaker similarity (sMOS), using a 9-point scale, ranging from 1 (inferior) to 5 (superior), with increments of 0.5 units. Results are presented with a confidence interval (CI) of 95%. Furthermore, we use the emotion mean opinion classification (eMOC) as suggested in [44]. For subjective evaluation, we randomly selected 10 sentences for each of the 5 emotions. These sentences were subsequently adapted to reflect each of the four different emotional states, resulting in a total of 200 samples, calculated as $10 \times 5 \times 4 = 200$.

2) *Objective Metrics*: For our objective evaluation, we incorporated a range of metrics: predicted mean opinion score, phoneme error rate (PER), character error rate (CER), word error rate (WER), emotion classification accuracy (ECA), and speaker embedding cosine similarity (SECS). The predicted MOS was assessed using UTMOS [64]⁶. For PER calculation, we employed a wav2vec2.0-based phoneme recognition model from Hugging Face [65]. CER and WER were determined using Whisper⁷ [66]. In assessing SECS, we extracted speaker embeddings from both the target and generated audio using

Resemblyzer⁸, subsequently computing their cosine similarity. This similarity measure ranges from -1 to 1, where higher values denote greater similarity. We evaluated the similarity for samples sharing the same speaker and emotion, then averaged these across all speakers. The objective evaluation of emotions in the generated speech was conducted using a pre-trained speech emotion recognition (SER) model [67]. Table I presents the results of each pre-trained rater model on the test set, comprising 1500 samples, for both ground-truth and vocoded samples. For an objective assessment, each of the 1500 test samples underwent transformation into the four other emotional states. This process resulted in a total of 6000 samples, calculated as $1500 \times 4 = 6000$.

D. Comparison Models

To benchmark the efficacy of our proposed method, we trained and compared it against several existing models:

- StarGAN-EVC⁹ [15]: This adversarial network model specializes in speech emotion conversion. Its GAN-based architecture supports parallel generation, distinguishing it in this domain.
- Seq2seq-EVC¹⁰ [21]: Employing a sequence-to-sequence (seq2seq) framework, this model adopts a two-stage strat-

⁸<https://github.com/resemble-ai/Resemblyzer>

⁹<https://github.com/glam-imperial/EmotionalConversionStarGAN>

¹⁰<https://github.com/KunZhou9646/seq2seq-EVC>

⁶<https://github.com/tarepan/SpeechMOS>

⁷<https://github.com/openai/whisper>

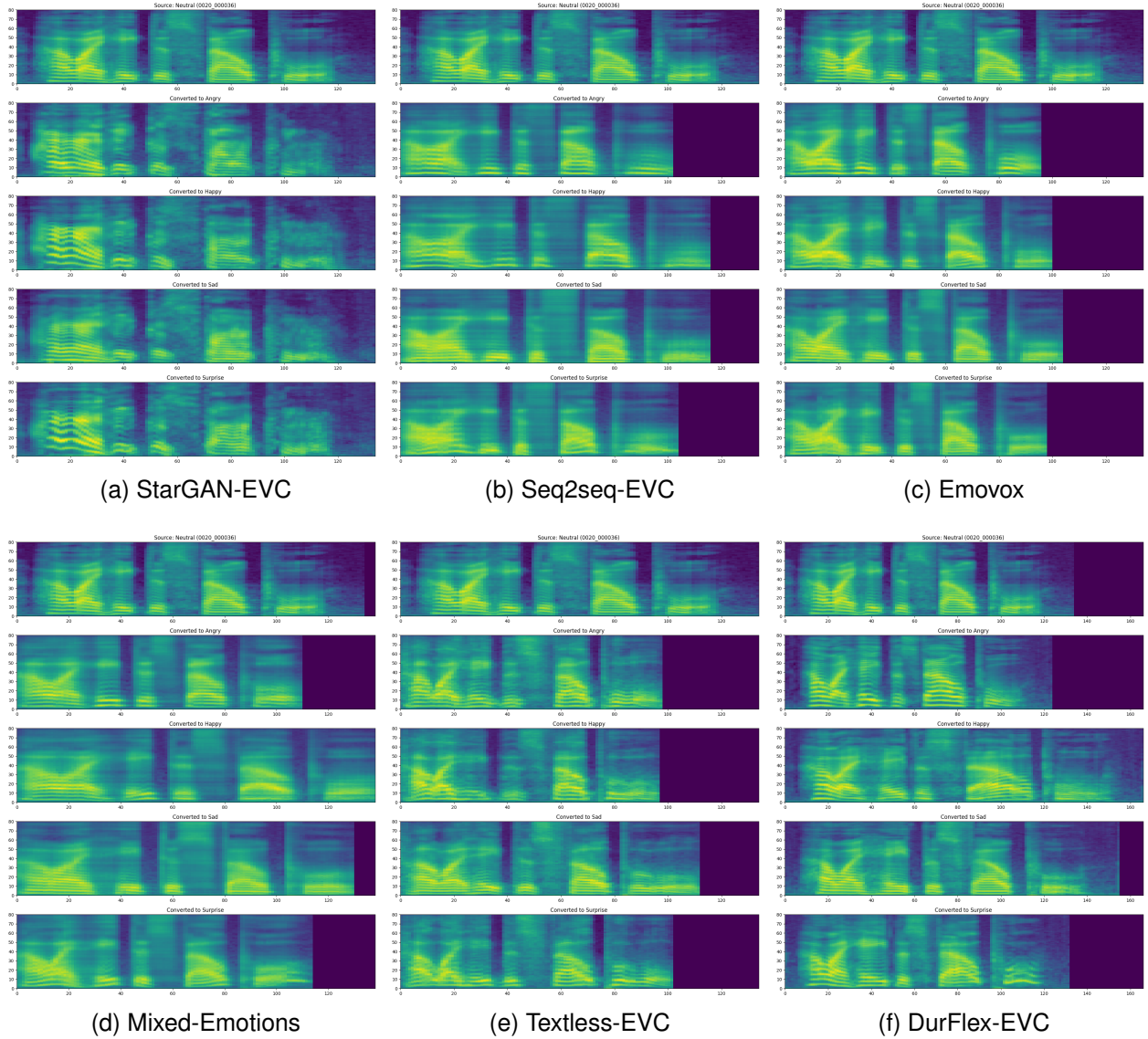


Fig. 5. Converted Mel-spectrogram results by emotion for each comparison model.

TABLE III
PREDICTED UNITS FOR EACH EMOTION.

Emotion	Unit sequence
Neutral (Source)	14 131 86 122 142 88 155 173 128 145 108 184 23 49 159 12 123 71 70 89 59 151 87 141 120 48 103 153 193 88 155 33 9 79 85 86 89 154 80 45 124 139 84 86 118 86 92
Angry	14 131 86 122 142 88 155 169 128 145 108 184 23 49 159 12 123 71 70 89 59 27 77 126 141 39 161 48 103 62 34 193 88 155 33 9 79 85 86 89 154 142 80 61 124 139 84 86 197 86 92
Happy	14 131 86 122 142 88 155 169 128 145 108 184 23 49 159 12 123 71 70 89 59 27 187 126 141 39 48 103 89 157 193 88 155 33 9 79 85 86 89 154 142 80 61 124 139 84 86 197 86 92
Sad	14 131 86 122 142 88 155 169 128 145 108 184 23 49 159 12 123 71 70 89 59 27 77 126 141 39 48 103 89 34 193 88 155 33 9 79 85 86 89 154 142 80 164 61 124 139 84 86 197 86 92 197 86 149 64 149 92
Surprise	14 131 86 122 142 88 155 169 128 145 108 184 23 49 159 12 123 71 70 89 59 27 187 126 141 39 48 103 59 193 88 155 33 9 79 85 86 89 154 142 80 61 124 139 84 86 197 86 92

egy utilizing the TTS model. A notable feature of the seq2seq-EVC is its capacity to jointly model duration and pitch.

- Emovox¹¹ [22]: Similar to Seq2seq-EVC, Emovox is based on a seq2seq structure. Its unique aspect lies in its focus on modulating emotional intensity. Emovox incorporates a ranking function to effectively model this intensity dimension.
- Mixed-Emotions¹² [68]: Operating on a seq2seq framework akin to Emovox, this model is designed for expressing mixed emotions. It shares the feature of controllable emotion intensity with Emovox.
- Textless-EVC¹³ [44]: This model approaches speech synthesis by deconstructing the speech signal into discrete learned representations. These include speech content

¹¹<https://github.com/KunZhou9646/Emovox>

¹²https://github.com/KunZhou9646/Mixed_Emotions

¹³https://github.com/facebookresearch/fairseq/tree/main/examples/emotion_conversion

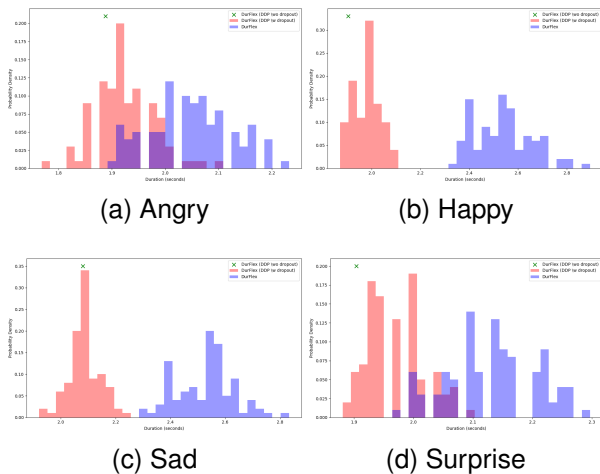


Fig. 6. Histogram of duration by emotion based on the structure of the duration predictor. X marks are DDP without dropouts, red bars are DDP with dropouts, and purple bars are models using SDP.

TABLE IV
COMPARISON RESULTS BASED ON THE STRUCTURE OF THE DURATION PREDICTOR.

Model	UTMOS (\uparrow)	PER (\downarrow)	CER (\downarrow)	WER (\downarrow)	ECA (\uparrow)	SECS (\uparrow)
DurFlex-EVC	3.58	17.31	8.26	20.75	91.58	74.83
DurFlex-EVC (w/ DDP)	3.39	17.60	8.59	21.56	90.09	72.94

units, prosodic features, speaker characteristics, and emotions. Each element is modified to align with the target emotion before being synthesized back into speech.

- **DurFlex-EVC:** Our proposed model encompasses a unit aligner, style autoencoder, stochastic duration predictor, hierarchical stylization encoder, and a diffusion-based generator. This model stands out with its comprehensive and integrated approach to emotional speech synthesis.

All comparison models were trained using the official implementations provided by their respective authors, ensuring consistency and reliability in the comparative analysis.

V. RESULT

A. Subjective and Objective Evaluation with Comparison Models.

We conducted both objective and subjective evaluations to assess the performance of our proposed model, comparing it with established baseline models. The outcomes of these evaluations, encompassing both comparison models and our proposed model, are meticulously detailed in Table II. Fig. 3 presents the confusion matrix for eMOC, and Fig. 4 illustrates the confusion matrix for ECA. The naturalness of the speech generated by our method, as indicated by the nMOS results, surpasses that of other models. This superiority is evident in our method’s ability to produce more naturally sounding speech. In the context of speaker similarity, our approach achieved the highest scores in both sMOS and SECS. Further, the results from eMOC and ECA demonstrate our method’s excellence not only in objective metrics but also in terms of perceptual quality. This dual success highlights the effectiveness of our method in capturing and reproducing

TABLE V
COMPARE DURATION DISTRIBUTIONS BY EMOTION BASED ON THE STRUCTURE OF THE DURATION PREDICTOR.

Model	Metrics	Emotion			
		Angry	Happy	Sad	Surprise
DurFlex-EVC w/ DDP (w/o dropout)	Mean	1.89	1.90	2.08	1.90
	Std	0	0	0	0
DurFlex-EVC w/ DDP (w/ dropout)	Mean	1.94	2.38	2.26	2.07
	Std	0.04	0.06	0.07	0.03
DurFlex-EVC	Mean	2.06	2.56	2.54	2.14
	Std	0.08	0.12	0.10	0.08

both the technical and experiential aspects of speech synthesis. Additionally, the ASR evaluation revealed that our method achieves lower values in PER, CER, and WER compared with other models. This indicates a superior pronunciation accuracy, highlighting our method’s proficiency in clear and accurate speech synthesis. These results collectively establish the effectiveness and superiority of our proposed method in various dimensions of speech synthesis.

B. Dynamics of Emotional Expression in Mel-Spectrogram Transformation

Fig. 5 illustrates the capabilities of each model in converting neutral speech into various emotional states. The performance differences among these models are notably distinct in their handling of speech duration and pitch variations, key elements in emotional speech synthesis. StarGAN-EVC, lacking support for duration variations, exhibited a consistent limitation: it generated outputs of uniform length regardless of the emotion being conveyed. This limitation was accompanied by instances of unnatural pitch in its speech output, detracting from the naturalness and emotional fidelity of the synthesis. Conversely, the autoregressive models—Seq2seq-EVC, Emovox, and Mixed-Emotions—demonstrated the capacity to produce outputs with varying durations. However, their synthesis was characterized by a noticeable smoothing effect, which potentially impacts the expressiveness and dynamism required for authentic emotional speech. Textless-EVC and DurFlex-EVC, both employing explicit duration modeling, were successful in generating outputs where durations aptly corresponded to the intended emotions. This feature is crucial for realistic emotional speech synthesis, as duration plays a significant role in conveying different emotional states. Our analysis concluded that the proposed method, presumably DurFlex-EVC, surpasses the other models in producing more natural and diverse speech representations. This superiority stems from its proficient handling of speech duration and pitch variations, essential factors in authentically replicating human emotional expression in speech synthesis. The results highlight our method’s advanced capability in this domain, setting a new benchmark for emotional speech synthesis.

C. Emotion-Responsive Unit

We developed the unit aligner to adjust contextually in response to varying emotions. Table III exemplifies the units our model predicts during the transformation of speech from a neutral to diverse emotional states. This demonstrates that our model assigns differential importance to speech units

contingent upon the intended emotion. In our research, it was determined that the prediction of distinct units, contingent on emotion, significantly enhanced the model’s capability in terms of expressiveness and pronunciation accuracy.

D. Evaluating Duration Prediction: Stochastic vs. Deterministic Approaches

To enhance duration diversity, we introduced a Stochastic Duration Predictor (SDP) and conducted a comparative analysis with a deterministic duration predictor (DDP). The DDP’s design adheres to the structure outlined in FastSpeech [47], encompassing two convolution layers, ReLU activation, layer normalization, and dropout.

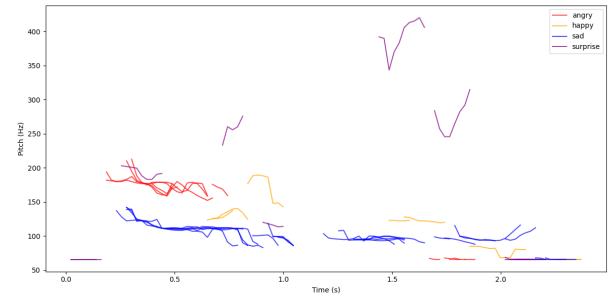
Numerous models [48], [49] employing explicit duration modeling have adopted this architecture, perceiving it as deterministic [58]. In alignment with this approach, we refer to it as the deterministic duration predictor (DDP) in our studies. However, our findings indicate that in practical applications, this structure does not exhibit deterministic behavior.

Fig. 6 presents a histogram depicting duration distributions derived from multiple conversions of the same speech sample. The red bars represent models utilizing DDP, while the blue bars signify models employing SDP. Notably, it was observed that DDP, influenced by the dropout layer, produces varying durations akin to those of SDP. Our investigations revealed that omitting the dropout layer from DDP consistently results in a fixed duration.

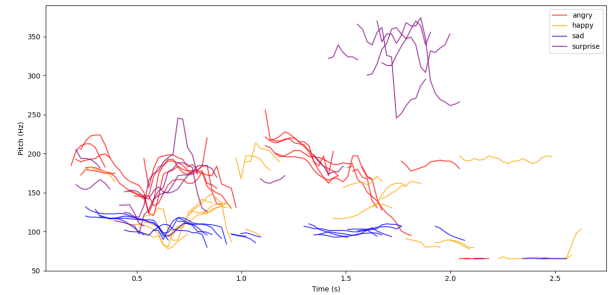
Table V displays the duration distributions for the DDP with and without dropout, as well as the SDP. The incorporation of dropout infuses randomness into the DDP. Additionally, SDP demonstrates a broader range of durations, attributed to its higher standard deviation compared to the variability induced by dropout in DDP. The performance of the model employing DDP is detailed in Table II, under DurFlex-EVC (w/ DDP). Comparative analysis reveals that the model utilizing SDP outperforms the DDP model across all evaluated metrics. This highlights the efficacy of SDP in generating precise durations for each emotional state, highlighting the critical role of accurate duration prediction in emotion conversion.

E. Diversity in Pitch

Our research findings indicate that utilizing a diffusion-based generator markedly enhances the quality and diversity of synthesized speech. We conducted a comparative analysis between a feed-forward transformer (FFT)-based decoder and a diffusion-based generator. Fig. 7 illustrates the pitch tracks of speech samples, each replicated five times per emotion, with pitch extraction performed using the YIN algorithm [69]. Fig. 7a, representing the FFT model, demonstrates a tendency towards producing a near-constant pitch across outputs. In contrast, the diffusion model, as depicted in Fig. 7b, yields a distinctly varied pitch in each iteration. Table VI details the performance metrics of both the FFT model (DurFlex-EVC (w/ FFT)) and the diffusion models (DurFlex-EVC). Although the FFT model, DurFlex-EVC (w/FFT), recorded lower CER and WER in comparison to DurFlex-EVC, it showed comparable results in terms of PER and SECS. However, it underperformed in the UTMOS and ECA.



(a) DurFlex-EVC w/ FFT



(b) DurFlex-EVC

Fig. 7. Pitch track of the same speech converted multiple times for each emotion (a) DurFlex-EVC with FFT decoder (b) DurFlex-EVC with diffusion-based decoder.

TABLE VI
COMPARISON OF RESULTS BASED ON THE STRUCTURE OF THE MEL-SPECTROGRAM GENERATOR.

Model	UTMOS (\uparrow)	PER (\downarrow)	CER (\downarrow)	WER (\downarrow)	ECA (\uparrow)	SECS (\uparrow)
DurFlex-EVC	3.58	17.31	8.26	20.75	91.58	74.83
DurFlex-EVC (w/ FFT)	3.03	17.32	7.42	19.41	62.07	73.17

TABLE VII
ABLATION STUDY.

Model	UTMOS (\uparrow)	PER (\downarrow)	CER (\downarrow)	WER (\downarrow)	ECA (\uparrow)	SECS (\uparrow)
DurFlex-EVC	3.58	17.31	8.26	20.75	91.58	74.83
w/o SAE	3.34	18.28	9.37	22.64	89.62	72.26
w/o unit loss	3.58	13.00	3.89	13.67	37.69	68.27
w/o UA	3.55	12.31	3.55	13.04	35.20	65.65
w/o UA and SAE	3.37	18.46	9.49	22.59	89.92	72.57

TABLE VIII
COMPARISON OF RESULTS BASED ON INPUT FEATURES.

Model	UTMOS (\uparrow)	PER (\downarrow)	CER (\downarrow)	WER (\downarrow)	ECA (\uparrow)	SECS (\uparrow)	BLEU (\uparrow)	UER (\downarrow)
w/ Mel-spec.	3.29	25.28	15.70	31.31	90.67	72.12	15.23	62.62
w/ linear-spec.	3.29	25.98	16.29	31.81	87.15	67.80	15.66	60.93
w/ wav2vec 2.0	3.34	30.55	21.46	38.44	92.17	66.61	11.96	62.67
w/ wavLM	3.36	23.44	12.07	26.22	92.08	67.07	25.51	46.43
w/ HuBERT	3.58	17.31	8.26	20.75	91.58	74.83	38.59	38.04

F. Compare Differences in Results based on Input Features.

In our study, we evaluated the efficacy of speech processing models using a range of input features. This comparison encompassed traditional signal processing features, such as Mel-spectrograms and linear spectrograms, alongside SSL features, including wav2vec 2.0 [26], wavLM [31], and HuBERT [28].

The comprehensive results of this evaluation are delineated in Table VIII.

Our analysis revealed notable variances in model performance contingent upon the chosen input features. Utilizing Mel-spectrograms led to enhanced ECA and SECS relative to the use of linear spectrograms. Conversely, models leveraging SSL features demonstrated superior UTMOS and ECA scores compared with those employing signal processing features. Within the SSL category, wav2vec 2.0 inputs were associated with diminished pronunciation proficiency, while wavLM inputs generally elevated performance across most metrics. Remarkably, the model utilizing HuBERT inputs exhibited superior performance in several metrics, with the exception of ECA.

We hypothesize that the superior performance of the HuBERT-based model can be attributed to its alignment with the target unit, which is a cluster of HuBERT features. This hypothesis was further substantiated by calculating both the BLEU score [70] and the unit error rate (UER). Our findings indicated a correlation between UER and pronunciation accuracy. These results underscore the critical importance of selecting appropriate input features to optimize the performance of speech processing models.

G. Ablation Study

In our research, we conducted an ablation study to validate the efficacy of our proposed method, which integrates a style autoencoder (SAE) for the decomposition and reconstruction of styles, and a unit aligner (UA) for effective modeling of both duration and context. The findings of this study are detailed in Table VII. The variant labeled “w/o SAE” employed a stylization transformer as opposed to a de-stylization transformer within the style autoencoder. The model denoted as “w/o unit loss” was trained in the absence of unit loss. Additionally, the “w/o UA” configuration processed the output of the style autoencoder using a hierarchical stylization encoder, incorporating unit-level grouping. The model “w/o UA and SAE” bypassed both the style autoencoder and unit aligner, generating Mel-spectrograms directly from units.

Our results revealed a decline in performance metrics when either the de-stylization transformer or the unit aligner was omitted, highlighting the crucial role of these components. Moreover, it was observed that the exclusion of unit loss during the training phase constrained the model to merely reconstruct the input speech, without executing the desired transformation. This emphasizes the significance of incorporating unit loss in training for achieving effective speech transformation.

H. Unseen Speaker Emotion Conversion

In our research, we expanded the scope of our experiments to apply our proposed model to scenarios involving unseen speakers. To facilitate this, we made specific modifications to the model’s structure: we replaced the speaker ID with speaker embeddings, which were extracted using the style encoder from Meta-StyleSpeech [71]. Additionally, we incorporated a gradient reversal layer (GRL) [72] and a linear layer into

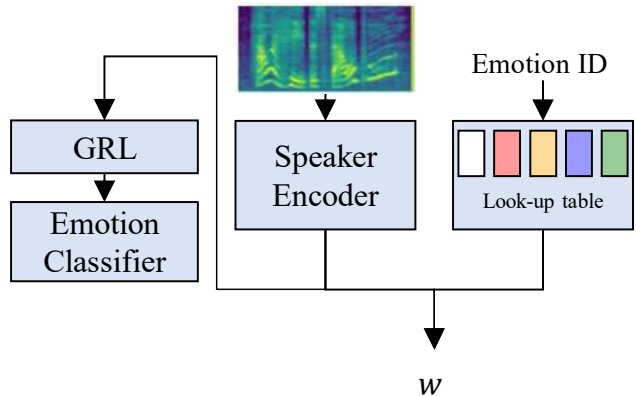


Fig. 8. Style embedding modeling for unseen speaker setting.

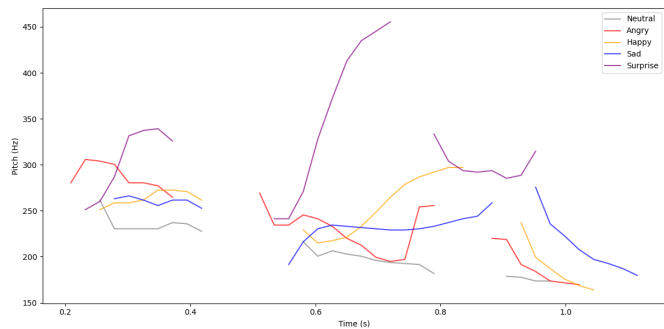


Fig. 9. Pitch track of converted speech on unseen speaker’s speech.

TABLE IX
EVALUATION RESULTS FOR SEEN AND UNSEEN SPEAKERS IN A SPEAKER ENCODER SETTING.

Model	UTMOS (\uparrow)	PER (\downarrow)	CER (\downarrow)	WER (\downarrow)	ECA	SECS (\uparrow)	eMOC
GT (Seen)	3.60	11.64	3.06	12.09	81.33	81.46	-
GT (Unseen)	4.03	10.07	0.67	1.39	-	83.77	-
Seen	3.44	16.72	7.75	20.16	79.17	65.70	69.39
Unseen	3.53	18.83	7.35	12.18	-	60.05	57.14

the style encoder to assist in emotion classification. This integration aids in simplifying the process of disentangling speaker and emotion characteristics. The function of the GRL’s emotion classification loss is to provide adversarial feedback, inhibiting the style encoder from assimilating emotional aspects. We assigned the weight for adversarial loss at 0.001, as our findings indicated a tendency for model collapse with increased weights in adversarial loss.

Fig. 8 illustrates the adapted style embedding technique for scenarios involving unseen speakers. The training process utilized the ESD dataset, while the VCTK dataset represented the unseen speakers. In our tests with unseen speakers, we randomly chose five sentences from each speaker in the VCTK dataset and transformed them to encompass all emotions.

Fig. 9 presents the pitch tracks resulting from the transformation of an unseen speaker’s voice across different emotions, showcasing the model’s capability to adapt emotions for new speakers. A neutral emotion is represented by a consistent and flat pitch. In contrast, emotions such as anger and happiness are characterized by elevated pitches with notable variations.

Sadness is reflected through lower pitch levels, and surprise is distinguished by the highest pitch peaks, indicative of the emotion’s abrupt nature.

Table IX contains the objective evaluations and eMOC scores for this specific speaker encoder setting. These findings validate that our model is capable of achieving emotion conversion without compromising quality or pronunciation accuracy in scenarios involving unseen speakers. Despite the success in emotional conversion, it was noted that preserving speaker similarity was less effectively achieved in these tests.

VI. DISCUSSION

Our model is influenced by the framework described in [73], which concentrates on modeling emotional pronunciation. Nonetheless, our methodology diverges substantially; whereas their model directly addresses pronunciation, our focus is on translating SSL features at the unit level. This perspective aligns more closely with the emotional translation mechanisms inherent in Textless-EVC [44]. The primary distinction in our approach lies in the utilization of the cross-attention output as the input for our model, rather than relying on the predicted units.

A. Limitations

Our model, utilizing diffusion-based structures, demonstrated enhanced expressiveness in the outputs, as evidenced in Fig. 7. However, a notable limitation of diffusion-based structures is their extensive computational demand and time intensive nature. We anticipate that this challenge will be alleviated by the advent of recent fast sampling methods [74].

The scope of our experiments also encompassed speaker generalization. While we successfully noted emotional transformations in the voices of unseen speakers, a discernible lack of speaker similarity was apparent, indicating a need for further refinement. Empirically, our observations suggest that models tested on unseen data often mirror the voice distribution of the data used for their pre-training. To enhance performance in zero-shot emotion conversion, we plan to expand the dataset.

In the configuration of our style autoencoder, we utilized MixLN for de-stylization and CLN for stylization. It was observed that the perturbations introduced by MixLN resulted in a compromise, affecting the equilibrium between expressiveness and pronunciation accuracy within our model. Moreover, the task of effectively separating style and content remains a formidable challenge in this domain, necessitating ongoing research and development to address this issue.

Our model, utilizing diffusion-based structures, demonstrated enhanced expressiveness in the outputs, as evidenced in Fig. 7. However, a notable limitation of diffusion-based structures is their extensive computational demand and time-intensive nature. We anticipate that this challenge will be alleviated by the advent of recent fast sampling methods [74].

B. Future Works

Contemporary research in the field of speech synthesis has progressively concentrated on the control of emotion

intensity. Various studies, such as those cited in [75] and [76], have adopted methodologies that involve modeling emotion intensity using ranking functions based on relative attributes. Alternatively, some research, as referenced in [77], has delved into modeling intensity through the interpolation of embeddings. This exploration is part of a broader array of innovative attempts, including those mentioned in [78] and [79], to manipulate emotion intensity in synthesized speech. While these studies have demonstrated the feasibility of modeling emotion intensity, a noticeable gap in achieving fine-grained control over this aspect remains. Addressing this gap is the focal point of our forthcoming research endeavors. Our future work is dedicated to developing more nuanced and sophisticated methods for controlling emotion intensity in speech synthesis. This advancement aims to bridge the current gap in the field, paving the way for more precise and varied emotional expression in synthetic speech.

VII. CONCLUSION

We have developed DurFlex-EVC, an innovative model for EVC, distinguished by its ability to generate speech with varying durations. This model incorporates a style autoencoder, which facilitates the decomposition and reconstruction of styles from input features. Additionally, the model employs a unit aligner that enables precise context modeling at the unit level. DurFlex-EVC is further enhanced by the inclusion of a stochastic duration predictor and a diffusion-based generator. This combination is instrumental in producing diverse speech outputs, tailored to specific emotional tones. Through rigorous experimental evaluations, DurFlex-EVC has demonstrated superiority over existing EVC models in terms of performance. We also expanded the application of our model to scenarios involving unseen speakers. In these extended experiments, DurFlex-EVC effectively converted emotions while maintaining high standards of speech quality and pronunciation accuracy. However, it encountered challenges in preserving speaker similarity. We posit that the duration modeling capability of DurFlex-EVC marks a significant leap forward in the domain of expressive voice conversion. This advancement unlocks new opportunities for creating realistic and dynamic speech synthesis, thereby contributing notably to the evolution of voice conversion technologies.

REFERENCES

- [1] N. Hussain, E. Erzin, T. M. Sezgin, and Y. Yemez, “Training Socially Engaging Robots: Modeling Backchannel Behaviors with Batch Reinforcement Learning,” *IEEE Trans. Affect. Comput.*, vol. 13, no. 4, pp. 1840–1853, 2022.
- [2] M. P. Aylett, A. Vinciarelli, and M. Wester, “Speech Synthesis for the Generation of Artificial Personality,” *IEEE Trans. Affect. Comput.*, vol. 11, no. 2, pp. 361–372, 2020.
- [3] C. Busso, M. Bulut, C.-C. Lee, A. Kazemzadeh, E. Mower, S. Kim, J. N. Chang, S. Lee, and S. S. Narayanan, “IEMOCAP: Interactive emotional dyadic motion capture database,” *Language resources and evaluation*, vol. 42, pp. 335–359, 2008.
- [4] A. Triantafyllopoulos, B. W. Schuller, G. İymen, M. Sezgin, X. He, Z. Yang, P. Tzirakis, S. Liu, S. Mertes, E. André, R. Fu, and J. Tao, “An Overview of Affective Speech Synthesis and Conversion in the Deep Learning Era,” *Proceedings of the IEEE*, vol. 111, no. 10, pp. 1355–1381, 2023.

- [5] F. Eyben, K. R. Scherer, B. W. Schuller, J. Sundberg, E. André, C. Busso, L. Y. Devillers, J. Epps, P. Laukka, S. S. Narayanan, and K. P. Truong, "The Geneva Minimalistic Acoustic Parameter Set (GeMAPS) for Voice Research and Affective Computing," *IEEE Trans. Affect. Comput.*, vol. 7, no. 2, pp. 190–202, 2016.
- [6] J. Sundberg, S. Patel, E. Bjorkner, and K. R. Scherer, "Interdependencies among Voice Source Parameters in Emotional Speech," *IEEE Trans. Affect. Comput.*, vol. 2, no. 3, pp. 162–174, 2011.
- [7] H. Ming, D. Huang, L. Xie, J. Wu, M. Dong, and H. Li, "Deep Bidirectional LSTM Modeling of Timbre and Prosody for Emotional Voice Conversion," in *Proc. Interspeech*, 2016, pp. 2453–2457.
- [8] Z. Du, B. Sisman, K. Zhou, and H. Li, "Expressive Voice Conversion: A Joint Framework for Speaker Identity and Emotional Style Transfer," in *2021 IEEE Automatic Speech Recognition and Understanding Workshop (ASRU)*, 2021, pp. 594–601.
- [9] R. Aihara, R. Takashima, T. Takiguchi, and Y. Arika, "GMM-based emotional voice conversion using spectrum and prosody features," *American Journal of Signal Processing*, vol. 2, no. 5, pp. 134–138, 2012.
- [10] J. Gao, D. Chakraborty, H. Tembine, and O. Olaleye, "Nonparallel Emotional Speech Conversion," in *Proc. Interspeech*, 2019, pp. 2858–2862.
- [11] K. Zhou, B. Sisman, M. Zhang, and H. Li, "Converting Anyone's Emotion: Towards Speaker-Independent Emotional Voice Conversion," in *Proc. Interspeech*, 2020, pp. 3416–3420.
- [12] K. Zhou, B. Sisman, and H. Li, "Vav-Gan For Disentanglement And Recomposition Of Emotional Elements In Speech," in *2021 IEEE Spoken Language Technology Workshop (SLT)*, 2021, pp. 415–422.
- [13] M. Elgaar, J. Park, and S. W. Lee, "Multi-Speaker and Multi-Domain Emotional Voice Conversion Using Factorized Hierarchical Variational Autoencoder," in *IEEE Int. Conf. Acoust., Speech, Signal Process.*, 2020, pp. 7769–7773.
- [14] F. Bao, M. Neumann, and N. T. Vu, "CycleGAN-Based Emotion Style Transfer as Data Augmentation for Speech Emotion Recognition," in *Proc. Interspeech*, 2019, pp. 2828–2832.
- [15] G. Rizos, A. Baird, M. Elliott, and B. Schuller, "Stargan for Emotional Speech Conversion: Validated by Data Augmentation of End-To-End Emotion Recognition," in *IEEE Int. Conf. Acoust., Speech, Signal Process.*, 2020, pp. 3502–3506.
- [16] J.-Y. Zhu, T. Park, P. Isola, and A. A. Efros, "Unpaired Image-To-Image Translation Using Cycle-Consistent Adversarial Networks," in *Proc. IEEE Int. Conf. Comput. Vis.*, Oct 2017.
- [17] Y. Choi, M. Choi, M. Kim, J.-W. Ha, S. Kim, and J. Choo, "StarGAN: Unified Generative Adversarial Networks for Multi-Domain Image-to-Image Translation," in *Proc. IEEE/CVF Conf. Comput. Vis. Pattern Recognit.*, June 2018.
- [18] J. Bao, D. Chen, F. Wen, H. Li, and G. Hua, "CVAE-GAN: Fine-Grained Image Generation Through Asymmetric Training," in *Proc. IEEE Int. Conf. Comput. Vis.*, Oct 2017.
- [19] C. Robinson, N. Obin, and A. Roebel, "Sequence-to-sequence Modelling of F0 for Speech Emotion Conversion," in *IEEE Int. Conf. Acoust., Speech, Signal Process.*, 2019, pp. 6830–6834.
- [20] T.-H. Kim, S. Cho, S. Choi, S. Park, and S.-Y. Lee, "Emotional Voice Conversion Using Multitask Learning with Text-To-Speech," in *IEEE Int. Conf. Acoust., Speech, Signal Process.*, 2020, pp. 7774–7778.
- [21] K. Zhou, B. Sisman, and H. Li, "Limited Data Emotional Voice Conversion Leveraging Text-to-Speech: Two-Stage Sequence-to-Sequence Training," in *Proc. Interspeech*, 2021, pp. 811–815.
- [22] K. Zhou, B. Sisman, R. Rana, B. W. Schuller, and H. Li, "Emotion Intensity and its Control for Emotional Voice Conversion," *IEEE Trans. Affect. Comput.*, vol. 14, no. 1, pp. 31–48, 2023.
- [23] B. van Niekerk, M.-A. Carbonneau, J. Zaïdi, M. Baas, H. Seuté, and H. Kamper, "A Comparison of Discrete and Soft Speech Units for Improved Voice Conversion," in *IEEE Int. Conf. Acoust., Speech, Signal Process.*, 2022, pp. 6562–6566.
- [24] H. Kim, S. Kim, J. Yeom, and S. Yoon, "UnitSpeech: Speaker-adaptive Speech Synthesis with Untranscribed Data," in *Proc. Interspeech*, 2023, pp. 3038–3042.
- [25] A. Baevski, Y. Zhou, A. Mohamed, and M. Auli, "wav2vec 2.0: A Framework for Self-Supervised Learning of Speech Representations," in *Proc. Adv. Neural Inf. Process. Syst.*, vol. 33. Curran Associates, Inc., 2020, pp. 12449–12460. [Online]. Available: https://proceedings.neurips.cc/paper_files/paper/2020/file/92d1e1eb1cd6f9fba3227870bb6d7f07-Paper.pdf
- [26] A. Baevski, S. Schneider, and M. Auli, "vq-wav2vec: Self-Supervised Learning of Discrete Speech Representations," in *Proc. Int. Conf. Learn. Representations*, 2020. [Online]. Available: <https://openreview.net/forum?id=rylwJxrYDS>
- [27] A. Babu, C. Wang, A. Tjandra, K. Lakhota, Q. Xu, N. Goyal, K. Singh, P. von Platen, Y. Saraf, J. Pino *et al.*, "XLS-R: Self-supervised cross-lingual speech representation learning at scale," *arXiv preprint arXiv:2111.09296*, 2021.
- [28] W.-N. Hsu, B. Bolte, Y.-H. H. Tsai, K. Lakhota, R. Salakhutdinov, and A. Mohamed, "HuBERT: Self-Supervised Speech Representation Learning by Masked Prediction of Hidden Units," *IEEE/ACM Trans. Audio, Speech, Lang. Process.*, vol. 29, pp. 3451–3460, 2021.
- [29] J. Devlin, M.-W. Chang, K. Lee, and K. Toutanova, "BERT: Pre-training of Deep Bidirectional Transformers for Language Understanding," in *Proceedings of the 2019 Conference of the North American Chapter of the Association for Computational Linguistics: Human Language Technologies, Volume 1 (Long and Short Papers)*. Minneapolis, Minnesota: Association for Computational Linguistics, Jun. 2019, pp. 4171–4186. [Online]. Available: <https://aclanthology.org/N19-1423>
- [30] K. Qian, Y. Zhang, H. Gao, J. Ni, C.-I. Lai, D. Cox, M. Hasegawa-Johnson, and S. Chang, "ContentVec: An Improved Self-Supervised Speech Representation by Disentangling Speakers," in *Int. Conf. on Mach. Learn.*, vol. 162. PMLR, 17–23 Jul 2022, pp. 18003–18017. [Online]. Available: <https://proceedings.mlr.press/v162/qian22b.html>
- [31] S. Chen, C. Wang, Z. Chen, Y. Wu, S. Liu, Z. Chen, J. Li, N. Kanda, T. Yoshioka, X. Xiao, J. Wu, L. Zhou, S. Ren, Y. Qian, Y. Qian, J. Wu, M. Zeng, X. Yu, and F. Wei, "WavLM: Large-Scale Self-Supervised Pre-Training for Full Stack Speech Processing," *IEEE J. Sel. Top. Signal Process.*, vol. 16, no. 6, pp. 1505–1518, 2022.
- [32] A. Baevski, W.-N. Hsu, Q. Xu, A. Babu, J. Gu, and M. Auli, "data2vec: A General Framework for Self-supervised Learning in Speech, Vision and Language," in *Int. Conf. on Mach. Learn.*, vol. 162. PMLR, 17–23 Jul 2022, pp. 1298–1312. [Online]. Available: <https://proceedings.mlr.press/v162/baevski22a.html>
- [33] J. Li, W. Tu, and L. Xiao, "Freevc: Towards High-Quality Text-Free One-Shot Voice Conversion," in *IEEE Int. Conf. Acoust., Speech, Signal Process.*, 2023, pp. 1–5.
- [34] S.-H. Lee, H.-Y. Choi, H.-S. Oh, and S.-W. Lee, "HierVST: Hierarchical Adaptive Zero-shot Voice Style Transfer," in *Proc. Interspeech*, 2023, pp. 4439–4443.
- [35] Z. Chen, S. Chen, Y. Wu, Y. Qian, C. Wang, S. Liu, Y. Qian, and M. Zeng, "Large-Scale Self-Supervised Speech Representation Learning for Automatic Speaker Verification," in *IEEE Int. Conf. Acoust., Speech, Signal Process.*, 2022, pp. 6147–6151.
- [36] S.-H. Lee, S.-B. Kim, J.-H. Lee, E. Song, M.-J. Hwang, and S.-W. Lee, "HierSpeech: Bridging the Gap between Text and Speech by Hierarchical Variational Inference using Self-supervised Representations for Speech Synthesis," in *Proc. Adv. Neural Inf. Process. Syst.*, vol. 35. Curran Associates, Inc., 2022, pp. 16624–16636. [Online]. Available: https://proceedings.neurips.cc/paper_files/paper/2022/file/69c754f571806bf15add18556ff39b4f-Paper-Conference.pdf
- [37] J. Wagner, A. Triantafyllopoulos, H. Wierstorf, M. Schmitt, F. Burkhardt, F. Eyben, and B. W. Schuller, "Dawn of the Transformer Era in Speech Emotion Recognition: Closing the Valence Gap," *IEEE Trans. Pattern Anal. Mach. Intell.*, vol. 45, no. 9, pp. 10745–10759, 2023.
- [38] A. Sivaraman and M. Kim, "Efficient Personalized Speech Enhancement Through Self-Supervised Learning," *IEEE J. Sel. Top. Signal Process.*, vol. 16, no. 6, pp. 1342–1356, 2022.
- [39] B. Irvin, M. Stamenovic, M. Kegler, and L.-C. Yang, "Self-Supervised Learning for Speech Enhancement Through Synthesis," in *IEEE Int. Conf. Acoust., Speech, Signal Process.*, 2023, pp. 1–5.
- [40] N. Zeghidour, A. Luebs, A. Omran, J. Skoglund, and M. Tagliasacchi, "SoundStream: An End-to-End Neural Audio Codec," *IEEE/ACM Trans. Audio, Speech, Lang. Process.*, vol. 30, pp. 495–507, 2022.
- [41] A. Défossez, J. Copet, G. Synnaeve, and Y. Adi, "High Fidelity Neural Audio Compression," *Transactions on Machine Learning Research*, 2023, featured Certification, Reproducibility Certification. [Online]. Available: <https://openreview.net/forum?id=ivCd8z8zR2>
- [42] D. Yang, J. Tian, X. Tan, R. Huang, S. Liu, X. Chang, J. Shi, S. Zhao, J. Bian, X. Wu *et al.*, "UniAudio: An Audio Foundation Model Toward Universal Audio Generation," *arXiv preprint arXiv:2310.00704*, 2023.
- [43] A. Polyak, Y. Adi, J. Copet, E. Kharitonov, K. Lakhota, W.-N. Hsu, A. Mohamed, and E. Dupoux, "Speech Resynthesis from Discrete Disentangled Self-Supervised Representations," in *Proc. Interspeech*, 2021, pp. 3615–3619.
- [44] F. Kreuk, A. Polyak, J. Copet, E. Kharitonov, T. A. Nguyen, M. Rivière, W.-N. Hsu, A. Mohamed, E. Dupoux, and Y. Adi, "Textless Speech Emotion Conversion using Discrete & Decomposed Representations," in *Proceedings of the 2022 Conference on Empirical Methods in Natural*

- Language Processing*. Abu Dhabi, United Arab Emirates: Association for Computational Linguistics, Dec. 2022, pp. 11 200–11 214. [Online]. Available: <https://aclanthology.org/2022.emnlp-main.769>
- [45] J. Shen, R. Pang, R. J. Weiss, M. Schuster, N. Jaitly, Z. Yang, Z. Chen, Y. Zhang, Y. Wang, R. Skerrv-Ryan, R. A. Saurous, Y. Agiomvrgianakis, and Y. Wu, “Natural TTS Synthesis by Conditioning Wavenet on MEL Spectrogram Predictions,” in *IEEE Int. Conf. Acoust., Speech, Signal Process.*, 2018, pp. 4779–4783.
- [46] N. Li, S. Liu, Y. Liu, S. Zhao, and M. Liu, “Neural Speech Synthesis with Transformer Network,” *Proc. AAAI Conf. Artif. Intell.*, vol. 33, no. 01, pp. 6706–6713, Jul. 2019. [Online]. Available: <https://ojs.aaai.org/index.php/AAAI/article/view/4642>
- [47] Y. Ren, Y. Ruan, X. Tan, T. Qin, S. Zhao, Z. Zhao, and T.-Y. Liu, “FastSpeech: Fast, Robust and Controllable Text to Speech,” in *Proc. Adv. Neural Inf. Process. Syst.*, vol. 32. Curran Associates, Inc., 2019. [Online]. Available: https://proceedings.neurips.cc/paper_files/paper/2019/file/f63f65b503e22cb970527f23c9ad7db1-Paper.pdf
- [48] Y. Ren, C. Hu, X. Tan, T. Qin, S. Zhao, Z. Zhao, and T.-Y. Liu, “FastSpeech 2: Fast and High-Quality End-to-End Text to Speech,” in *Proc. Int. Conf. Learn. Representations*, 2021. [Online]. Available: <https://openreview.net/forum?id=piLPYqxtWuA>
- [49] J. Kim, S. Kim, J. Kong, and S. Yoon, “Glow-TTS: A Generative Flow for Text-to-Speech via Monotonic Alignment Search,” in *Proc. Adv. Neural Inf. Process. Syst.*, vol. 33. Curran Associates, Inc., 2020, pp. 8067–8077. [Online]. Available: https://proceedings.neurips.cc/paper_files/paper/2020/file/5c3b99e8f92532e5ad1556e53ceea00c-Paper.pdf
- [50] C.-c. Yeh, P.-c. Hsu, J.-c. Chou, H.-y. Lee, and L.-s. Lee, “Rhythm-Flexible Voice Conversion Without Parallel Data Using Cycle-GAN Over Phoneme Posteriorgram Sequences,” in *2018 IEEE Spoken Language Technology Workshop (SLT)*, 2018, pp. 274–281.
- [51] K. Tanaka, H. Kameoka, T. Kaneko, and N. Hojo, “ATTS2S-VC: Sequence-to-sequence Voice Conversion with Attention and Context Preservation Mechanisms,” in *IEEE Int. Conf. Acoust., Speech, Signal Process.*, 2019, pp. 6805–6809.
- [52] S.-H. Lee, H.-R. Noh, W.-J. Nam, and S.-W. Lee, “Duration Controllable Voice Conversion via Phoneme-Based Information Bottleneck,” *IEEE/ACM Trans. Audio, Speech, Lang. Process.*, vol. 30, pp. 1173–1183, 2022.
- [53] Z. Yang, X. Jing, A. Triantafyllopoulos, M. Song, I. Aslan, and B. W. Schuller, “An Overview & Analysis of Sequence-to-Sequence Emotional Voice Conversion,” in *Proc. Interspeech*, 2022, pp. 4915–4919.
- [54] M. Chen, X. Tan, B. Li, Y. Liu, T. Qin, sheng zhao, and T.-Y. Liu, “AdaSpeech: Adaptive Text to Speech for Custom Voice,” in *Proc. Int. Conf. Learn. Representations*, 2021. [Online]. Available: <https://openreview.net/forum?id=Drynvt7gg4L>
- [55] R. Huang, Y. Ren, J. Liu, C. Cui, and Z. Zhao, “GenerSpeech: Towards Style Transfer for Generalizable Out-Of-Domain Text-to-Speech,” in *Proc. Adv. Neural Inf. Process. Syst.*, vol. 35. Curran Associates, Inc., 2022, pp. 10970–10983. [Online]. Available: https://proceedings.neurips.cc/paper_files/paper/2022/file/4730d10b22261faa9a95ebf7497bc556-Paper-Conference.pdf
- [56] A. Vaswani, N. Shazeer, N. Parmar, J. Uszkoreit, L. Jones, A. N. Gomez, L. u. Kaiser, and I. Polosukhin, “Attention is All you Need,” in *Proc. Adv. Neural Inf. Process. Syst.*, vol. 30. Curran Associates, Inc., 2017. [Online]. Available: https://proceedings.neurips.cc/paper_files/paper/2017/file/3f5ee243547dee91fbd053c1c4a845aa-Paper.pdf
- [57] M. Kang, D. Min, and S. J. Hwang, “Grad-StyleSpeech: Any-Speaker Adaptive Text-to-Speech Synthesis with Diffusion Models,” in *IEEE Int. Conf. Acoust., Speech, Signal Process.*, 2023, pp. 1–5.
- [58] J. Kim, J. Kong, and J. Son, “Conditional Variational Autoencoder with Adversarial Learning for End-to-End Text-to-Speech,” in *Int. Conf. on Mach. Learn.*, vol. 139. PMLR, 18–24 Jul 2021, pp. 5530–5540. [Online]. Available: <https://proceedings.mlr.press/v139/kim21f.html>
- [59] V. Popov, I. Vovk, V. Gogoryan, T. Sadekova, and M. Kudinov, “Grad-TTS: A Diffusion Probabilistic Model for Text-to-Speech,” in *Int. Conf. on Mach. Learn.*, vol. 139. PMLR, 18–24 Jul 2021, pp. 8599–8608. [Online]. Available: <https://proceedings.mlr.press/v139/popov21a.html>
- [60] K. Zhou, B. Sisman, R. Liu, and H. Li, “Emotional voice conversion: Theory, databases and ESD,” *Speech Communication*, vol. 137, pp. 1–18, 2022. [Online]. Available: <https://www.sciencedirect.com/science/article/pii/S0167639321001308>
- [61] I. Loshchilov and F. Hutter, “Decoupled Weight Decay Regularization,” in *Proc. Int. Conf. Learn. Representations*, 2019. [Online]. Available: <https://openreview.net/forum?id=Bkg6RiCqY7>
- [62] S. gil Lee, W. Ping, B. Ginsburg, B. Catanzaro, and S. Yoon, “BigVGAN: A Universal Neural Vocoder with Large-Scale Training,” in *The Eleventh Proc. Int. Conf. Learn. Representations*, 2023. [Online]. Available: https://openreview.net/forum?id=iTtGCMDEzS_
- [63] H. Zen, V. Dang, R. Clark, Y. Zhang, R. J. Weiss, Y. Jia, Z. Chen, and Y. Wu, “LibriTTS: A Corpus Derived from LibriSpeech for Text-to-Speech,” in *Proc. Interspeech*, 2019, pp. 1526–1530.
- [64] T. Saeki, D. Xin, W. Nakata, T. Koriyama, S. Takamichi, and H. Saruwatari, “UTMOS: UTokyo-SaruLab System for VoiceMOS Challenge 2022,” in *Proc. Interspeech*, 2022, pp. 4521–4525.
- [65] Q. Xu, A. Baevski, and M. Auli, “Simple and Effective Zero-shot Cross-lingual Phoneme Recognition,” in *Proc. Interspeech*, 2022, pp. 2113–2117.
- [66] A. Radford, J. W. Kim, T. Xu, G. Brockman, C. Mcleavey, and I. Sutskever, “Robust Speech Recognition via Large-Scale Weak Supervision,” in *Int. Conf. on Mach. Learn.*, vol. 202. PMLR, 23–29 Jul 2023, pp. 28 492–28 518. [Online]. Available: <https://proceedings.mlr.press/v202/radford23a.html>
- [67] Y. Li, T. Zhao, and T. Kawahara, “Improved End-to-End Speech Emotion Recognition Using Self Attention Mechanism and Multitask Learning,” in *Proc. Interspeech*, 2019, pp. 2803–2807.
- [68] K. Zhou, B. Sisman, R. Rana, B. W. Schuller, and H. Li, “Speech Synthesis with Mixed Emotions,” *IEEE Trans. Affect. Comput.*, pp. 1–16, 2022.
- [69] A. de Cheveigné and H. Kawahara, “YIN, a fundamental frequency estimator for speech and music,” *J. Acoust. Soc. Am.*, vol. 111, no. 4, pp. 1917–1930, 04 2002. [Online]. Available: <https://doi.org/10.1121/1.1458024>
- [70] K. Papineni, S. Roukos, T. Ward, and W.-J. Zhu, “BLEU: A Method for Automatic Evaluation of Machine Translation,” in *Proceedings of the 40th Annual Meeting on Association for Computational Linguistics*, ser. ACL ’02. USA: Association for Computational Linguistics, 2002, p. 311–318. [Online]. Available: <https://doi.org/10.3115/1073083.1073135>
- [71] D. Min, D. B. Lee, E. Yang, and S. J. Hwang, “Meta-stylespeech : Multi-speaker adaptive text-to-speech generation,” in *Int. Conf. on Mach. Learn.*, vol. 139. PMLR, 18–24 Jul 2021, pp. 7748–7759. [Online]. Available: <https://proceedings.mlr.press/v139/min21b.html>
- [72] Y. Ganin and V. Lempitsky, “Unsupervised Domain Adaptation by Backpropagation,” in *Int. Conf. on Mach. Learn.*, vol. 37. Lille, France: PMLR, 07–09 Jul 2015, pp. 1180–1189. [Online]. Available: <https://proceedings.mlr.press/v37/ganin15.html>
- [73] M. Tahon, G. Lecorvé, and D. Lolive, “Can We Generate Emotional Pronunciations for Expressive Speech Synthesis?” *IEEE Trans. Affect. Comput.*, vol. 11, no. 4, pp. 684–695, 2020.
- [74] Z. Xiao, K. Kreis, and A. Vahdat, “Tackling the Generative Learning Trilemma with Denoising Diffusion GANs,” in *Proc. Int. Conf. Learn. Representations*, 2022. [Online]. Available: <https://openreview.net/forum?id=JprMOp-q0Co>
- [75] X. Zhu, S. Yang, G. Yang, and L. Xie, “Controlling Emotion Strength with Relative Attribute for End-to-End Speech Synthesis,” in *2019 IEEE Automatic Speech Recognition and Understanding Workshop (ASRU)*, 2019, pp. 192–199.
- [76] Y. Lei, S. Yang, and L. Xie, “Fine-Grained Emotion Strength Transfer, Control and Prediction for Emotional Speech Synthesis,” in *2021 IEEE Spoken Language Technology Workshop (SLT)*, 2021, pp. 423–430.
- [77] S.-Y. Um, S. Oh, K. Byun, I. Jang, C. Ahn, and H.-G. Kang, “Emotional Speech Synthesis with Rich and Granularized Control,” in *IEEE Int. Conf. Acoust., Speech, Signal Process.*, 2020, pp. 7254–7258.
- [78] C.-B. Im, S.-H. Lee, S.-B. Kim, and S.-W. Lee, “EMOQ-TTS: Emotion Intensity Quantization for Fine-Grained Controllable Emotional Text-to-Speech,” in *IEEE Int. Conf. Acoust., Speech, Signal Process.*, 2022, pp. 6317–6321.
- [79] Y. Guo, C. Du, X. Chen, and K. Yu, “Emodiff: Intensity Controllable Emotional Text-to-Speech with Soft-Label Guidance,” in *IEEE Int. Conf. Acoust., Speech, Signal Process.*, 2023, pp. 1–5.